ION BEAM PROPAGATION STABILITY IN A LINAC ACCELERATING CHANNEL BASED ON COMBINED RF-FOCUSING

S.S. Tishkin, M.G. Shulika, O.M. Shulika
National Science Center "Kharkov Institute of Physics and Technology", Kharkiv, Ukraine
E-mail: tishkin@kipt.kharkov.ua

The issue of simultaneous longitudinal and transverse particle propagation stability in a linear ion accelerator channel based on combined RF-focusing is investigated. Values for RFQ field gradient to provide transverse propagation stability for all the particles in an acceleration mode are calculated. It is also shown that electrical strength of the electrodes influences the gradient value. Much attention is given to modeling of an accelerating-focusing channel which provides the minimal growth in beam emittance.

PACS: 29.17.+w

INTRODUCTION

A new line of investigation in accelerator physics and technology based on a possibility to steadily accelerate charged particles by the RF field has been evolving since the early 1960s owing to studies by V. Vladimirsky [1], M. Good [2], Ya. Fainberg [3], and many others. In particular, V. Vladimirsky suggested making use of the RF quadruple field to stabilize radially charged particle as they are being accelerated in a self-focusing accelerator. M. Good and Ya. Fainberg independently proposed that the use of periodically alternating reference phase improves radial-phase stability of the accelerated beam. These two principals initiated the development of RF-focusing in ion linacs in two different ways: RF quadrupole focusing (RFQ) and alternating phase focusing (APF). A modified version of the APF method (MAPF) is described in Ref. [4]. As an initial part of the MILAC machine (see Ref. [5]), the MAPF-based accelerator with built-up field along the grouping section and stepwise variations in the reference particle phase along the focusing section was designed, constructed, and put into operation Refs. [6 - 8]. Ref. [9] presents the accelerating and focusing channel of a medium-energy proton linac that uses the combination of axisymmetrical and quadrupole gaps for particle acceleration and focusing. A general principle for the RF-field focusing of particles namely combined RF focusing (CRFF) with the mass-to-charge ratio $A/q \le 65$ is proposed in Ref. [10]. Further improvements on the MILAC accelerator such as replacement of grid and magnetic quadrupole focusing for CRFF are presented in Refs. [11, 12]. Design, layout, and adjustment procedures for interdigital IH accelerating CRFF-based structures for the MILAC machine are discussed in Refs. [13 - 18].

This paper objective is to develop a mathematical model that enables calculation of general parameters of the focusing gap providing stable beam acceleration with high acceleration rate and low emittance growth.

MATHEMATICAL MODEL. GENERAL EQUATIONS

To examine the problem of simultaneous longitudinal and transverse accelerated beam stability in a CRFF-based channel, let us use the approach described by I. Kapchinskij in Ref. [19]. The space-charge influence on beam dynamics is considered negligible. The problem is approached in the following way: first, the area of phase particle capture into the acceleration process is determined; then, the prospect of stable radial motion of these particles is evaluated, and if it is the case, the required values for field gradient along the accelerating channel are calculated.

As has been stated above, the combination of axisymmetrical and quadrupole gaps constitutes a CRFF-based accelerating channel. The longitudinal equations of particle motion are as in Refs. [19, 20].

$$\frac{d\psi}{dt} = -(\omega/\gamma_s^2)h\,,$$

$$\frac{d}{dt}(\beta_s p_s h) = eE\beta_s\left[\cos(\varphi_s+\psi)-\cos\varphi_s\right]. \quad (1)$$

Here $\psi = \varphi - \varphi_s$ is the phase shift relative to the reference particle, ω is the operating RF frequency, $\gamma = (1-\beta^2)^{-1/2}$, $h = \left(p - p_s\right)/p_s$, p_s is the reference particle impulse, e is the elementary charge, and E is traveling wave amplitude.

For Eqs. (1) there is a corresponding Hamiltonian

$$H = -\frac{\omega}{2p_s\beta_s\gamma_s^2}p_\psi^2 + eE\beta_s\left[\psi\cos\varphi_s - \sin(\varphi_s+\psi)\right] \quad (2)$$

with $p_\psi = \beta_s p_s h$.

The second term in Eq. (2) is similar to the potential function and determines the domain of stable particle motion by the interval $\varphi_s \le \psi \le -2\varphi_s$ yielding the value of $3|\varphi_s|$.

When considering stability of radial motion, we assume the change in particle velocity and phase shift is negligible. The linearized transverse motion equations are as in Ref. [19]

$$\frac{d^2x}{d\tau^2} + \Psi_x^2(\tau)x = 0\,, \quad \frac{d^2y}{d\tau^2} + \Psi_y^2(\tau)y = 0\,, \quad (3)$$

where $\Psi_x^2(\tau)$ and $\Psi_y^2(\tau)$ is the coefficient of unit period, i.e. $\Psi_{x,y}^2(\tau) = \Psi_{x,y}^2(\tau+1)$.

The linear equations Eqs. (3) are referred to as Mathieu-Hill equations and provide a basis for the analysis of particle motion in a strong-focusing channel. To study motion stability along a focusing period, the application of matrix algebra methods seems most convenient.

So, as the variables in Eqs. (3) can be split, we consider only one equation and rewrite it in the matrix form

$$\begin{pmatrix} x \\ dx/d\tau \end{pmatrix}_{\tau+1} = \begin{pmatrix} T_{11} & T_{12} \\ T_{21} & T_{22} \end{pmatrix} \begin{pmatrix} x \\ dx/d\tau \end{pmatrix}_{\tau}.$$

Here the matrix T called the matrix of the focusing period links the variable and its derivative at the beginning and the end of the focusing period which starts at any given phase τ in the range from 0 to 1 ($0 \le \tau \le 1$).

The advantages of the matrix method over the direct use of differential equations for description of particle dynamics lie in the following: generally, a focusing line consists of various sections (namely, an accelerating gap, a drift segment, a quadrupole lens, etc.) and each such section is described by a corresponding differential equation. So, each section has its own transformation matrix for particle coordinates and velocities which is defined regardless of initial conditions at the beginning of the section. Thus, the overall matrix for the whole focusing line is the product of all section matrices. By calculating the coefficients of the matrix T, we completely define particle motion along the section under investigation.

The stable trajectory domain in the strong-focusing channel is defined by

$$\left|\left(T_{11}+T_{22}\right)/2\right| < 1.$$

In our case the CRFF-based section consists of three distinctive segments, namely, the drift gap, the axisymmetrical accelerating one, and the RF quadrupole one.

The Drift Gap Matrix. Let us assume that there is no field over the distance h. Then the corresponding matrix takes the form

$$H = \begin{pmatrix} 1 & h/L \\ 0 & 1 \end{pmatrix} \quad (4)$$

with L being the length of the whole focusing section.

The Matrix for the Axisymmetrical Accelerating Gap in a Standing Wave System. Let us use the electric field component E_z along the accelerating gap in the "square wave" approximation which means that the electric field along the gap is constant and has the value of E_g while inside the drift tube it equals zero. At the beginning and the end of the gap there is a transit region of length Δz over which the change in radial velocity occurs (over the main part of the gap radial motion is drift-like). Thus, the overall matrix for the accelerating gap is the product of three matrices:

$$\Gamma = \begin{pmatrix} 1 & 0 \\ \gamma_2 & 1 \end{pmatrix} \begin{pmatrix} 1 & g/L \\ 0 & 1 \end{pmatrix} \begin{pmatrix} 1 & 0 \\ \gamma_1 & 1 \end{pmatrix}. \quad (5)$$

Here the first and the third matrix describes the trajectory refraction with corresponding coefficient γ_1 and γ_2 (by definition $\gamma = 1/x\,\Delta\left(dx/d\tau\right)$ and the middle matrix represents the idle segment of length g.

Now, let us calculate the velocity change at the beginning (or the end) of the segment.

The general equation of motion for the longitudinal coordinate (assuming it x) is

$$\ddot{x} - \frac{1}{2}\Omega_q{}^2(t)x = 0, \quad (6)$$

where

$$\Omega_q{}^2 = \frac{e}{m_0}\frac{\partial E_z}{\partial z}. \quad (7)$$

By substituting Eq. (7) into Eq. (6), we rewrite the latter in a difference form as

$$\frac{\Delta\upsilon_{input}}{\Delta t} = -\frac{1}{2}\frac{e}{m}\frac{\Delta E_g\left(-\frac{g}{2}\right)}{\Delta z}x,$$

$$\frac{\Delta\upsilon_{output}}{\Delta t} = \frac{1}{2}\frac{e}{m}\frac{\Delta E_g\left(\frac{g}{2}\right)}{\Delta z}x$$

for the input and output segments respectively.

Then, the expression for the trajectory refraction takes the form

$$\frac{\Delta\upsilon_{input}}{x} = -\frac{1}{2}\frac{e}{m}\frac{\Delta t}{\Delta z}E_g\left(-\frac{g}{2}\right),$$

$$\frac{\Delta\upsilon_{output}}{x} = \frac{1}{2}\frac{e}{m}\frac{\Delta t}{\Delta z}E_g\left(\frac{g}{2}\right).$$

After introducing a dimensionless variable, τ and assuming $\upsilon_s \simeq \Delta z/\Delta t$, we obtain the refraction coefficients as

$$\gamma_1 = -\frac{eL}{2m_0c^2\beta_s^2}E_g\cos\left(-\frac{\omega g}{2\upsilon_s}+\varphi\right),$$

$$\gamma_2 = \frac{eL}{2m_0c^2\beta_s^2}E_g\cos\left(\frac{\omega g}{2\upsilon_s}+\varphi\right).$$

Here φ represents the standing wave phase at the moment of the particle crossing the accelerating gap center.

The Matrix for the RF quadrupole section. The transverse motion equations are

$$\frac{d^2x}{dt^2} = \frac{e}{m_0}\frac{\partial E_x}{\partial x}(z)\cos\omega t\cdot x,$$

$$\frac{d^2y}{dt^2} = \frac{e}{m_0}\frac{\partial E_y}{\partial y}(z)\cos\omega t\cdot y$$

with the quadrupole field component accounted for (see Ref. [19]).

After introducing a function for the quadrupole field gradient

$$G(x,y,z) = \frac{1}{2}\left[\frac{\partial E_x}{\partial x}(x,y,z) - \frac{\partial E_y}{\partial y}(x,y,z)\right]$$

and allowing for

$$\frac{\partial E_x}{\partial x} + \frac{\partial E_x}{\partial x} = -\frac{\partial E_z}{\partial z},$$

we obtain

$$\frac{\partial E_x}{\partial x} = -\frac{1}{2}\frac{\partial E_z}{\partial z} + G, \qquad \frac{\partial E_y}{\partial y} = -\frac{1}{2}\frac{\partial E_z}{\partial z} - G. \quad (8)$$

The term $-1/2\left(\partial E_z/\partial z\right)$ in both Eqs. (8) describes the defocusing effect of the axisymmetrical rf field in an accelerating gap. As we are considering the focusing effect over the quadrupole section, we assume this term infinitesimal in relation to the quadrupole rf field gradient. In addition, we also assume the particle displacement over the gap length is small (the so-called thin lens approximation). Then, the resulting matrix is

$$Q=\begin{pmatrix}1 & l_q/2L\\ 0 & 1\end{pmatrix}\begin{pmatrix}1 & 0\\ \gamma_q & 1\end{pmatrix}\begin{pmatrix}1 & l_q/2L\\ 0 & 1\end{pmatrix}. \qquad (9)$$

Here l_q is the quadrupole gap length, γ_q is the refraction coefficient. The matrixes to the left and right correspond to the drift segments while the matrix in the center describes the refraction of particle trajectory. All the particles crossing the refraction line, experience a change in their velocity

$$\Delta\frac{dx}{dt}=\frac{e}{m_0}x\int_{l_q}G(z)\cos\omega t(z)\frac{dz}{\upsilon},$$
$$\Delta\frac{dy}{dt}=-\frac{e}{m_0}y\int_{l_q}G(z)\cos\omega t(z)\frac{dz}{\upsilon}. \qquad (10)$$

Assuming the value of υ does not change over the quadrupole segment and introducing a dimensionless variable, $\tau=\upsilon t/L$ we obtain the following expressions

$$\Delta\frac{dx}{d\tau}=\frac{eL}{m_0c^2}x\int_{l_q}G(z)\cos\omega t(z)\frac{dz}{\upsilon},$$
$$\Delta\frac{dy}{d\tau}=-\frac{eL}{m_0c^2}y\int_{l_q}G(z)\cos\omega t(z)\frac{dz}{\upsilon}.$$

Allowing for $t(z)=z/\upsilon+\varphi/\omega$ and the function $G(z)$ to be even, the expressions for the refraction coefficients take the form

$$1/x\left(\Delta dx/d\tau\right)=eL/m_0\upsilon^2\cos\varphi\int_{l_q}G(z)\cos\left(2\pi z/\beta\lambda\right)dz,$$
$$1/y\left(\Delta dy/d\tau\right)=-eL/m_0\upsilon^2\cos\varphi\int_{l_q}G(z)\cos\left(2\pi z/\beta\lambda\right)dz.$$

If we represent the integrand as

$$\int_{l_q}G(z)\cos\left(2\pi z/\beta\lambda\right)dz=\left(\frac{\int_{l_q}G(z)\cos\left(2\pi z/\beta\lambda\right)dz}{\int_{l_q}G(z)dz}\right)\int_{l_q}G(z)dz$$

then the following function

$$T_q=\int_{l_q}G(z)\cos\left(2\pi z/\beta\lambda\right)dz\Big/\int_{l_q}G(z)dz$$

presents a similarity to the transit time in case of an axisymmetric gap between drift tubes. On putting the function $G(z)$ constant and equal to G_0 over the segment of length g_q where the so-called 'horned' electrodes overlap, we arrive at the expression

$$T_q=\sin\left(\pi g_q/\beta\lambda\right)\Big/\left(\pi g_q/\beta\lambda\right).$$

Thus, the refraction coefficients take the form

$$1/x\left(\Delta dx/d\tau\right)=eL/m_0\upsilon^2\cos\varphi\,G_0T_qg_q,$$
$$1/y\left(\Delta dy/d\tau\right)=-eL/m_0\upsilon^2\cos\varphi\,G_0T_qg_q.$$

So, the matrixes for all the segments of a CRFF-based focusing section have been defined completely. These matrixes will be useful while considering particle motion stability for a CRFF-based focusing structure of various designs. As an example, let us consider a section consisting of double rf quadrupole segments separated by three axisymmetrical gaps. This structure has a FOOODDOOOF pattern (with F being the focusing segment in a transverse plane, O representing the axisymmetrical gap, and D standing for the defocusing area). The schematic view of the structure is given in Fig. 1,b,d.

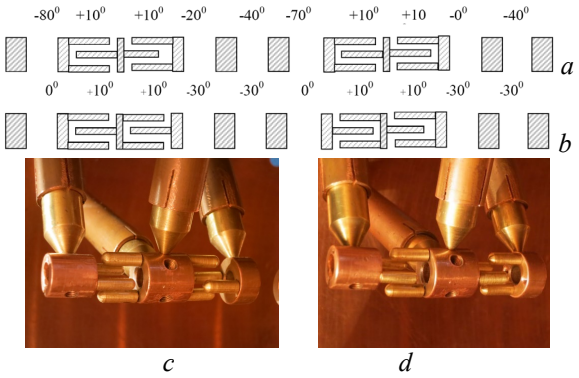

Fig. 1. Focusing sections of a CRFF-based structure: two focusing sections incorporating rf quadrupole doublets and respective reference particle phases – the schematic view (a) and the corresponding section of the real machine (c); medium-energy focusing section with the use of double rf quadrupoles and relevant reference particle phases – the schematic view (b) and the real section (d)

The combined matrix for the whole section under consideration is the product of all segment matrixes

$$M=1/2\,HQH\Gamma H\Gamma H\Gamma H\bar{Q}H\bar{Q}H\Gamma H\Gamma H\Gamma HQ\,1/2\,H.$$

Here H is the drift gap matrix (see Eq. (4)), Q is the quadrupole segment matrix (see Eq. (9)), $\bar{Q}$ is the matrix Q with the refraction coefficient $-\gamma_q$, and Γ is the matrix of the axisymmetrical gap between drift tubes (see Eq. (5)). In general, the segment length, i.e. quadrupole, axisymmetrical, or idle one, can take on different values for each segment in the section.

As has been pointed out, the condition $\varphi_s\le\psi\le-2\varphi_s$ determines the domain of particle capture for the channel under consideration and gives the size of this domain the value of $3|\varphi_s|$. At medium energy, the reference particle phase usually lies in the range of –30°…–20°. So, we assume all the particles whose phase lies in the range of –30°…+60° are localized in the region where radial stability occurs. The condition for radial stability is

$$1/2\left|Sp\,M\right|=\left|\cos\mu\right|=\left|\left(T_{11}+T_{22}\right)/2\right|<1$$

with $Sp\,M$ denoting the matrix spur, $\cos\mu$ representing cosine of the radial phase incursion along the focusing part, T_{11} and T_{22} being the diagonal elements of the combined matrix.

Next, setting the particles to be protons, the operating frequency to 350 MGz, the energy to 3 MeV, and the maximum electric field strength to 180 kV/cm, and using the expressions for the matrix T and the stability condition, we can obtain the minimal gradient value that ensures all the particles at the phase range of -30°…+60° are localized in the radial stability area. Fig. 2 presents the dependence of the radial phase incursion on the particle transit phase over the focusing period at G_0 =220 kV/cm^2. It is clear from the figure, all the particles at the mentioned above phase range and the given value of the quadrupole gradient are located in the radial stability region.

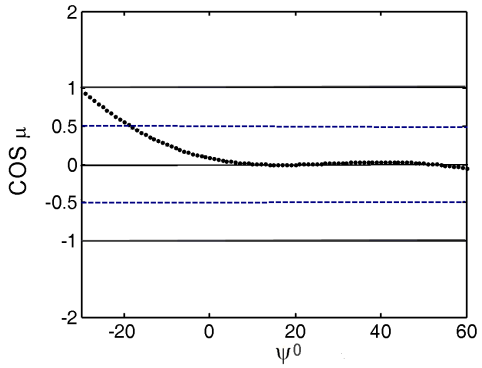

Fig. 2. Radial phase shift calculated for the focusing segment's matrix

RESULTS AND DISCUSSION

Notice that the "square wave" approximation has been applied to calculate fields over the axisymmetrical gaps and field gradients over the quadrupole ones. This approach does not allow the real electrode configuration to be accounted for and thus, a question "Is it possible to obtain the necessary value for the quadrupole gradient providing sufficient electrical strength of the quadrupole gap?" remains open.

However, there is for any channel calculated by the "square wave" approximation a corresponding channel of actual configuration. And a quadrupole gap to be equivalent in focusing terms to a quadrupole segment matrix Q, the following condition

$$\int_{l_q} G(z)\cos\left(2\pi z/\beta\lambda\right)dz = G_0 T_q g_q \qquad (11)$$

must be satisfied.

Let us set up a problem as follows: It is required to find out quadrupole electrode geometry and potential difference between these electrodes in order (i) to satisfy the equivalence condition Eq. (11); (ii) to maximize the channel aperture; (iii) to provide sufficient electrical strength of the gap.

It is generally agreed that an accelerating gap features electrical strength if the condition $E_s \le (2...3)K_p$ is fulfilled. Here E_s is the maximal electric field intensity on the electrode surface, K_p is Kilpatrick criterion. If we set the operation frequency to 350 MHz, then K_p=183 kV/cm.

The optimization problem has been dealt with by means of RFQFLD code which is a part of our software environment to develop accelerating and focusing channels based on rf field focusing (see Ref. [10]). To calculate fields in an actual structure, the code RFQFLD implements a method of auxiliary charges. According to this method, a quasi-static field potential is a superposition of elementary point charges placed outside the calculated domain. Boundary conditions on the surface in N points give the quantity to N charges. The charge inside an electrode is specified by charge density. Fig. 3 depicts the field potential distribution in a quadrupole gap cross-section for the given geometry. In the graph, black dots correspond to the auxiliary charges while circles represent observation points on the electrode surface. It is obvious from Fig. 4 that the quadrupole gradient function $G(z)$ describing the actual electrode geometry reaches its maximum at 214 kV/cm^2 in the middle of the gap.

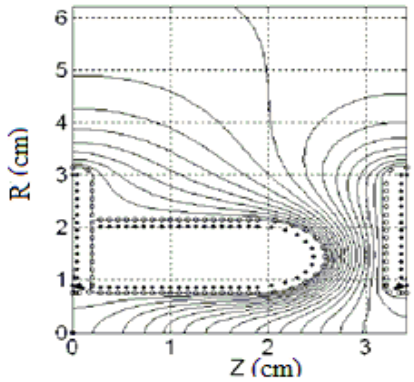

Fig. 3. Electrode geometry and field potential distribution in the gap cross-section

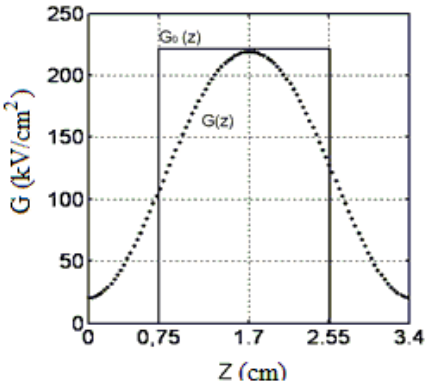

Fig. 4. Quadrupole gradient function $G(z)$ for geometry on Fig. 3 and its 'square wave' counterpart $G_0(z)$

The boundary conditions are as follows

$$\left.\frac{\partial\varphi}{\partial z}\right|_{z=0} = 0;\ \left.\frac{\partial\varphi}{\partial z}\right|_{z=l_q} = 0;\ \varphi|_{r\to\infty} = 0;\ \varphi_1 = -62.5\ kV;\ \varphi_2 = 62.5\ kV$$

with l_q being the quadrupole segment length, $r = \sqrt{x^2 + y^2}$, φ_1 and φ_2 are the respective potentials on the left and right drift tube.

The main parameters obtained in numerical calculations are: the quadrupole segment length $l_q = \beta\lambda/2$ =3.4 cm, the channel aperture is 0.75 cm, outer radius of the drift tube equals to 3.2 cm, the ratio of the quadrupole electrode radius to the minimal distance between the electrode and the channel axis $R_e/R_0 = 1$, the distance between the 'horned' electrode and the opposite drift tube end is 0.6 cm, and maximal electric field intensity is 356 kV/cm (=1.94 K_p).

Hence, this demonstrates the feasibility of the rf field focusing. It is also worth pointing out that the accelerating segment used in calculations is very short and measures $\beta\lambda/2$ =3.4 cm. This means that the maximal field is concentrated at the end of the 'horned' electrode. With increase in particle velocity, the distance between the quadrupole electrode and the opposite drift tube varies ~β. This, in turn, allows the potential difference across the accelerating gap to be increased along with the channel aperture. The chosen limit for electrical strength criterion of $2K_p$ is usually applied in assess-

ment of surface electrical field intensity in an initial part of accelerator (IPA). The fact is that inside the IPA the electrode surface becomes contaminated by ion source operation resulting in impairment of electrode electrical strength in due course. The next accelerator part, the intermediate, is free from such problem and the criterion limit can be increased up to $3K_p$.

In our calculations, the reference particle phase is φ_s =+15°. This choice is dictated by the following: the quadrupole gap influence is proportional to $\cos\varphi$ with maximal effect taking place at $\varphi = 0$. If $\varphi_s > 0$, the stability area expands by shifting to negative reference phases. This is valid for negligible changes in the phase shift over the focusing period. But at small and medium particle velocities, phase fluctuations can significantly influence the radial motion.

Figs. 5 and 6 present the phase portrait and the phase shift of radial oscillations for a monoenergetic beam with zeroth reference phase at the quadrupole segments calculated for different number of focusing gaps by APFRFQ0 code (see Ref. [10]).

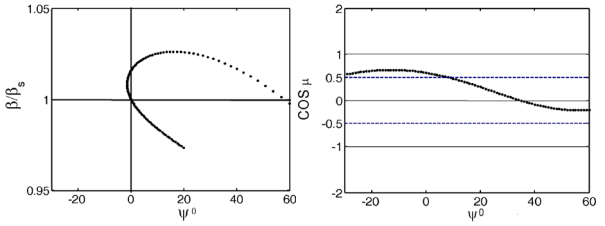

a *b*

Fig. 5. Phase portrait (a) and phase incursion of particle radial oscillations (b) in the first focusing period. Transverse particle oscillations are included into consideration

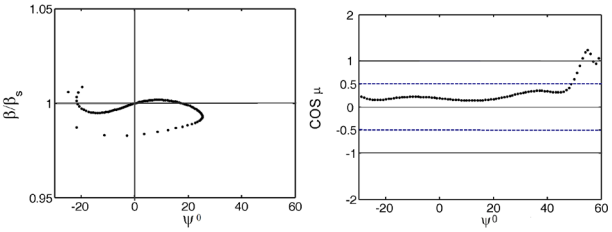

a *b*

Fig. 6. Phase portrait (a) and phase incursion of particle radial oscillations (b). Four focusing periods. Transverse particle oscillations are included into consideration

As illustrated in Figs. 5 and 6, transverse and longitudinal particle oscillation coupling over several focusing periods results in "smoothing" of phase shift that constitutes one of the conditions for minimal emittance growth during acceleration process. It should be also remarked that the angle of particle capture into the acceleration process in this case is no less $3|\varphi_s|$ as has been calculated before.

The CRFF-based accelerating channel can also be used as an initial part of linac. Due to the fact that the frequency of phase oscillations is maximal at low velocities, the focusing section has the different pattern ODFOOO (see Fig. 1,a,c) where focusing alternating elements follow each other (contrary to the previous pattern). By applying the built-up electric field across the accelerating gap and simultaneously reducing the reference phase magnitude, it is possible to capture into acceleration process no less 50% of beam particles with transverse particle motion stability ensured. Fig. 7 shows the phase portrait and the phase shift of radial oscillations for a monoenergetic A/q=4 (He^+) beam at the end of the accelerating section.

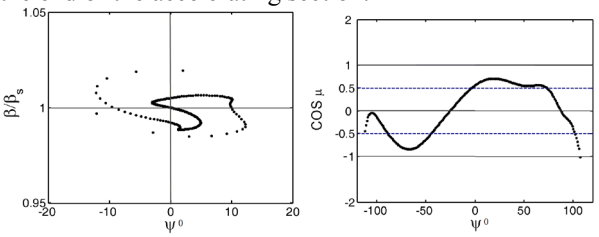

a *b*

Fig. 7. Phase portrait (a) and phase incursion of particle radial oscillations (b) at the acceleration section exit. Transverse particle oscillations are included into consideration. Mass-to-charge ration is A/q=4, output energy is 1 MeV/nucl

The main parameters in this case are: energy ranges from 0.03 MeV/nucl. up to 1 MeV/nucl., the channel length is 2 m, the number of accelerating gaps – 25, the number of focusing segments – 5, the maximal field intensity is 90 keV/cm. As Fig. 7 states, the acceptance angle is about 220°, the phase extent is no more than 30° at the structure exit, and all the particles captured into acceleration process lie the area of radial stability.

CONCLUSIONS

Performed the analytical and numerical studies into radial-phase motion stability in the CRFF-based channel have demonstrated that:

– the combined rf focusing is universal and can be used for light as well as heavy particle acceleration at medium energy;

– to accelerate charged particle bunches already formed, the focusing structure with the double quadrupole gaps and the axisymmetrical accelerating segments in-between is preferable. The example pattern for such structure is FOOODDOOOF. The accelerating and focusing channel of this type can provide radial stability for all the particles captured into the acceleration process, minor emittance growth and smaller electric field strength on the surface of the quadrupole electrodes if compared with the channel of ODFOOO pattern;

– the accelerating and focusing channel with ODFOOO pattern is suitable for a charged particle bunch formation and its acceleration without preliminary grouping. Such channel provides the acceptance angle of about 220° for stable acceleration.

REFERENCES

1. V.V. Vladimirsky. Variant hard focusing in linear accelerator // *PTE*. 1956, №3, p. 35-36.
2. M.L. Good. Phase-Reversal focusing in Linear Accelerators // *Phys. Rev*. 1953, №2, p. 538.
3. Ya.B. Fainberg. Alternating phase focusing // *Proc. of Intern. Symposium on High Energy Accelerators and Pion Physics*. Geneva: CERN, 1956, v. 1, p. 91.
4. V.G. Papkovich, N.A. Khizhnyak, N.G. Shulika. Alternating phase focusing in a linear ion accelerator

// *Problems of Atomic Science and Technology*. 1978, № 2, p. 51-56.
5. V.A. Bomko, A.M. Yegorov, B.V. Zaytsev, et al. Development of the MILAC complex for nuclear physical investigations // *Problems of Atomic Science and Technology. Series "Nuclear Physics Investigations"*. 2006, № 3, p. 100-104.
6. V.A. Bomko, A.P. Kobets, Z.E. Ptukhina, S.S. Tishkin. Variant alternation phase focusing with step change of the synchronous phase // *Problems of Atomic Science and Technology. Series "Nuclear Physics Investigations"*. 2004, № 2, p. 153-154.
7. V.O. Bomko, Z.O. Ptukhina, S.S. Tishkin. Variant of the accelerating and focusing structure of the high current linear ion accelerator // *Problems of Atomic Science and Technology. Series "Nuclear Physics Investigations"*. 2006, № 2, p. 163-165.
8. V.O. Bomko, O.F. Dyachenko, Ye.V. Ivakhno, et al. New prestripping section of the MILAC linear accelerator designed for accelerating a high current beam of light ions // *Proc. of EPAC 2006 Edinburgh, Scotland*. 2006, p. 1627-1629.
9. V.O. Bomko, Z.E. Ptukhina, S.S. Tishkin, N.G. Shulika. Variant of focusing by an accelerating RF field in linear ion accelerators // *Proc. RUPAC-2002*. Obninsk, 2002, v. 1, p. 227-230.
10. S.S. Tishkin. Combined focusing by RF-field for ion linac accelerators // *The Journal of Kharkiv National University. Physical Series "Nuclear, Particle, Fields"*. 2008, № 808, Issue 2(38), p. 37-46.
11. S.S. Tishkin. Accelerating channel for initial section of heavy ion linear accelerator with combined high-frequency focusing // *Problems of Atomic Science and Technology*. 2008, № 4, p. 327-331.
12. B.V. Zajtsev, S.S. Tishkin, N.G. Shulika. The prospects for combined high-frequency focusing usage in high-current heavy ion linacs // *Problems of Atomic Science and Technology. Series "Nuclear Physics Investigations"*. 2010, № 3, p. 85-89.
13. S.S. Tishkin, A.F. Dyachenko, B.V. Zajtsev, et al. Accelerating structure with combined radio-frequency focusing for acceleration of heavy ions A/q≤20 to energy 1 MeV/u // *Problems of Atomic Sience and Technology. Series "Nuclear Physics Investigations"*. 2018, № 3, p. 8-11.
14. A.F. Dyachenko, B.V. Zaytsev, S.S. Tishkin, et al. An accelerating and focusing structure with combined RF focusing for heavy ion accelerator // *Problems of Atomic Science and Technology. Series "Nuclear Physics Investigations"*. 2014, № 3, p. 16-19.
15. V.O. Bomko, B.V. Zajtsev, J.V. Ivakhno, et al. Accelerating structure with radio-frequency quadrupole (RFQ) for the heavy ions accelerating // *Problems of Atomic Science and Technology. Series "Nuclear Physics Investigations"*. 2010, № 3, p. 26-30.
16. A.F. Dyachenko, B.V. Zaytsev, S.S. Tishkin, et al. An accelerating & focusing structure with combined RF focusing for heavy ion accelerator // *Problems of Atomic Science and Technology. Series "Nuclear Physics Investigations"*. 2014, № 3, p. 16-19.
17. V.O. Bomko, A.F. Dyachenko, B.V. Zajtsev, et al. Experimental modelling of the hybrid accelerating structure of heavy ion linear accelerator // *Problems of Atomic Science and Technology. Series "Nuclear Physics Investigations"*. 2016, № 3, p. 17-20.
18. V.O. Bomko, A.F. Dyachenko, B.V. Zajtsev, et al. Regulation of level RF field in hybrid structures of heavy ions linear accelerator // *Problems of Atomic Science and Technology. Series "Nuclear Physics Investigations"*. 2016, № 3, p. 21-25.
19. I.M. Kapchinskij. *Dynamics of particles in ion linear resonant accelerators*. M.:«Atomizdat», 1966, 310 p.
20. B.P. Murin, B.I. Bondarev, V.V. Kushin, A.P. Fedorov. *Ion linear accelerators*: *V.1. Problems and theory* / Edited by B.P. Murin. M.: «Atomizdat», 1978, 264 p.

Article received 08.10.2019

УСТОЙЧИВОСТЬ ДВИЖЕНИЯ ИОННЫХ ПУЧКОВ В УСКОРЯЮЩИХ КАНАЛАХ ЛИНЕЙНЫХ УСКОРИТЕЛЕЙ С КОМБИНИРОВАННОЙ ВЫСОКОЧАСТОТНОЙ ФОКУСИРОВКОЙ

С.С. Тишкин, Н.Г. Шулика, О.Н. Шулика

Исследован вопрос обеспечения одновременной продольной и поперечной устойчивости движения частиц в каналах линейных ускорителей ионов с комбинированной высокочастотной фокусировкой. Определены значения градиентов высокочастотного квадрупольного поля, при которых обеспечивается поперечная устойчивость для всех частиц, захваченных в режим ускорения по фазовому движению. Показано, что эти значения можно обеспечить в квадрупольных зазорах при соблюдении электрической прочности электродов. Особое внимание уделено построению ускоряюще-фокусирующих каналов с минимальным ростом эмиттанса пучка в процессе ускорения.

СТІЙКІСТЬ РУХУ ІОННИХ ПУЧКІВ У КАНАЛАХ, ЩО ПРИСКОРЮЮТЬ, ЛІНІЙНИХ ПРИСКОРЮВАЧІВ З КОМБІНОВАНИМ ВИСОКОЧАСТОТНИМ ФОКУСУВАННЯМ

С.С. Тішкін, М.Г. Шуліка, О.М. Шуліка

Досліджено питання забезпечення одночасної повздовжньої та поперечної стійкості руху частинок у каналах лінійних прискорювачів іонів з комбінованим високочастотним фокусуванням. Визначені значення градієнтів високочастотного квадрупольного поля, при яких забезпечується поперечна стійкість для всіх частинок, що захоплені в режим прискорення по фазовому руху. Показано, що ці значення можна забезпечити в квадрупольних зазорах при виконанні умов електричної міцності електродів. Особлива увага приділена побудові каналів, що прискорюють та фокусують, з мінімальним ростом емітанса пучка при прискоренні.